

Applications of BOTDR fiber optics to the monitoring of underground structures

Ricardo A. Moffat ^{*}, Juan F. Beltran ^a and Ricardo Herrera ^b

Department of Civil Engineering, University of Chile, Blanco Encalada 2002, Santiago 8370449, Chile

(Received December 17, 2013, Revised December 31, 2014, Accepted May 11, 2015)

Abstract. Three different applications for monitoring displacements in underground structures using a BOTDR-based distributed optical fiber strain sensing system are presented. These applications are related to the strain measurements of (1) instrumented PVC tube designed to be attached to tunnel side wall and ceiling as a sensor; (2) rock bolts for tunnels; and (3) shotcrete lining under loading. The effectiveness of using the proposed strain sensing system is evaluated by carrying out laboratory tests, in-situ measurements, and numerical simulations. The results obtained from this validation process provide confidence that the optical fiber is able to quantify strain fields under a variety of loading conditions and consequently use this information to estimate the behavior of rock mass during mining activity. As the measuring station can be located as far as 1 km of distance, these alternatives presented may increase the safety of the mine during mining process and for the personnel doing the measurements on the field.

Keywords: displacement sensors; mining; tunnels; instrumentation; optical fiber

1. Introduction

The analysis of rock mechanics problems in mining is one of the most challenging issues in Geotechnical Engineering. These issues include stresses that are extremely high, rock properties that are difficult to obtain and a large volume of rock that has to be prospected considering budgetary restrictions often found in underground mining. This together with the dangerous consequences of a failure involving loss of life and economic return create a need for increasing accuracy and reliability in the monitoring of underground tunnels.

The structural monitoring of underground constructions can significantly improve the safety of operational practices and the evaluation of the stability and properties of the rock mass. By regularly providing the information on the structural and functional conditions of the underground structure, monitoring can help prevent local failures, detect problems and their locations, and carry out maintenance and repairs operations in time. Hence, maintenance cost is optimized and economic losses are decreased. The most frequent methods for geotechnical measurements are inclinometers, extensometers and LVDTs. Recently new technologies have been proposed to measure displacement. For example, Shimizu *et al.* (2014) have used Global Positioning Systems

^{*}Corresponding author, Ph.D., Assistant Professor, E-mail: rmoffatc@ing.uchile.cl

^a Ph.D., Assistant Professor, E-mail: jbeltran@ing.uchile.cl

^b Ph.D., Assistant Professor, E-mail: riherrer@ing.uchile.cl

(GPS) using a relative positioning method with an accuracy of millimeters over an extensive area.

The use of optical fiber seems to be a promising alternative to monitor underground structures because it allows for detailed monitoring of long extensions using a single sensor. Optical fibers have been successfully used to monitor strain and temperature in rock masses (Gage *et al.* 2013), as well as strain, temperature, and leakage in pipelines (Inaudi and Glisic 2010). Regarding tunnel applications, Naruse *et al.* (2007) developed a monitoring system using a BOTDR-based distributed optical fiber strain sensing system that was used in a field trial in an underground ventilation tunnel for six months to monitor deformation due to mining activities. The monitoring system consisted of optical fiber sensors attached to the tunnel ceiling and sidewall through the use of rock bolts driven into the tunnel at intervals of 3 m, in which one sensor unit comprised five spans (15 m). Similarly, Cheung *et al.* (2010) examined the feasibility of using BOTDR for monitoring the joint movements of concrete tunnel lining in an existing London Underground tunnel. Optical fiber was installed along the tunnel lining and the movements were captured by measuring the strains of the fiber attached across the segment joints. Based on the results of the field trial conducted, it was concluded that, coupled with other monitoring tools (such as pore pressure sensors and thermal sensors for the concrete segments) the continuous strain distribution provided by the BOTDR can be useful for investigating the tunnel lining response. Mohamad *et al.* (2012) presented a study of a field trial of BOTDR fiber optic monitoring of a segmental bolted tunnel lining. Deformations induced in the tunnel lining were caused by an adjacent excavation for the construction of a second tunnel at a distance less than one tunnel diameter apart. The optical fiber was attached to the tunnel lining using the point-fixing method. BOTDR measurements were validated by comparisons with results given by extensometers and analytical methods (based on the differential equation for a circular arch).

The principle of BOTDR (Brillouin Optical Time Domain Reflectometer) consists in measuring the change in frequency of the light traveling on an optical fiber that is subjected to strain. Fig. 1 illustrates qualitatively the effect on the frequency of the reflected light when the optical fiber is subjected to strain changes. The idea is simple but the equipment is very sophisticated, as it is required to measure in short (few meters) and long (few kilometers) distances the change in frequency of light. This light is transmitted by the equipment (BOTDR) through the optical fiber and is reflected back so that changes in frequency can be observed. The theory behind the technology is presented in Horiguchi *et al.* (1989), and a summary of its implementation for particular applications can be found in Ohno *et al.* (2001), Thévenaz *et al.* (1998), and Hao and Wu (2008). These last authors used this technology to monitor cracks in concrete structural elements, and concluded that the fiber had to be looped in the element in order to improve the accuracy of the strain and crack detection. More recently, Sun *et al.* (2014) used BOTDR sensing technology successfully to monitor corrosion induced cracking in a concrete column.

The main advantages of this technique with respect to other sensors when applied to a mining environment are (Nikles *et al.* 2005, Naruse *et al.* 2007).

- It allows the monitoring of strains at long distances
- It withstands extreme temperatures
- It is impervious to electromagnetic interference
- It does not suffer oxidation or problems with water
- It measures strains in the range of 0.01% to 1%, along the optical fiber.

In addition, because the equipment can be far away from the location being measured, measurements can be obtained up until the failure of tunnels (for example in block caving) and

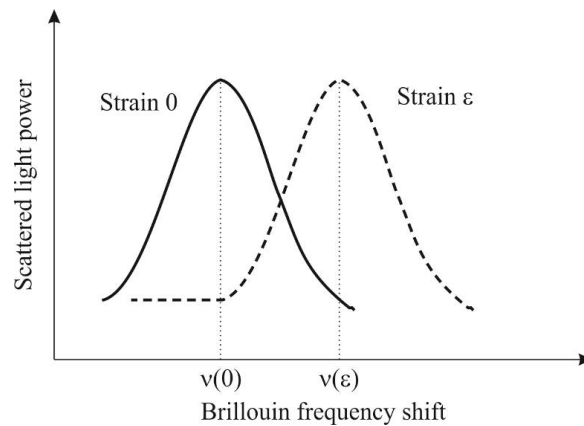


Fig. 1 Change in frequency of the reflected light when subjected to strain

create alert systems in future zones of the mine. These advantages are the drivers for the exploration of other potential applications of BOTDR to mining and tunnel monitoring.

In this paper, three applications of strain measurements, based on optical fiber sensors that are read by the BOTDR equipment (N8510 optical fiber strain sensing system from Advantest) are presented: (1) use of instrumented PVC tube attached to the sidewall and roof of a mining tunnel; (2) in rock-bolts (anchors) for tunnels; and (3) the use of optical fiber to measure the deformation of shotcrete under loading. Laboratory and field measurements are taken for the first two applications, and laboratory tests and numerical simulations under different loading conditions are performed for the third technique. For both laboratory and field strain measurements, the sensing fiber used is nylon coated standard single-mode optical fiber with a diameter of 0.9 mm and strain resolution equal to 0.01%. All three applications showed adequate performance and, therefore, constitute a useful tool worth of consideration in the monitoring of rock tunnels, especially in a mining environment. More specifically, the PVC tube sensor shows its ability to deduce displacement of its support points in the order of 5 and 60 mm. The anchor system shows its ability to detect strains in the order of 0.02% and infer the actual safety state of the anchor. Finally, the optical fiber used in the shotcrete allows the detection of deformations from the moment when the shotcrete starts to develop cracks until the point of failure. With these data it is possible to define an adequate strain associated to a level of absorbed energy of the shotcrete.

2. Measurement of displacements in rock tunnels

2.1 Description of the sensor

The proposed sensor is designed to measure longitudinal strains due to bending deformation induced by the relative displacements of its supports which are rigidly connected to the rock mass. In this particular study, the proposed sensor tube (ST) is supported in four points: A, B, P1, and P2 in Fig. 2 which correspond to the attachment locations of the sensor to the rock mass. As such, if the ST is installed in a region where the rock mass locally displaces (within ST length), relative displacements of the same amount are induced to the ST supports due to their rigid connections to

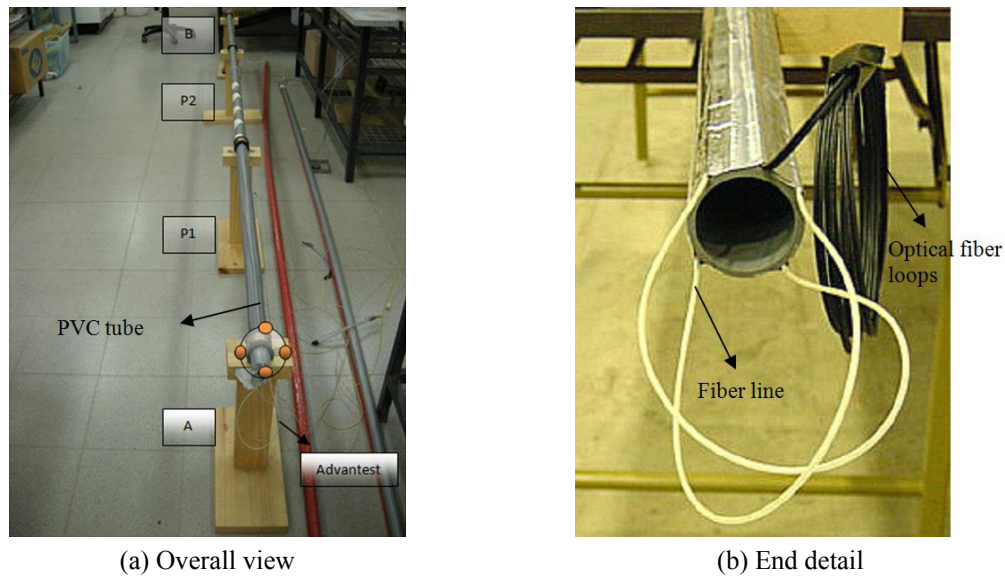


Fig. 2 Sensor tube configuration

the rock mass. The geometrical parameters of the tubes (i.e., length, thickness and diameter) are selected on the basis of bending behavior of the tubes (slenderness ratio) and ease of transportation, handling, and installation in both laboratory and the field. In addition, the slenderness of the ST determines the magnitude of the relative displacement values of the ST supports necessary to induce axial strain levels greater than a threshold value defined by the error measurement associated to the optical fiber as later discussed in the paper.

PVC tubes of 5.0 m length and 25 and 40 mm external diameters were used for the laboratory and field tests. Standard properties of the PVC used (Duratec, Vinilit) are: rupture tensile stress equal to 50 MPa, elasticity modulus of 3.000 MPa, and axial failure strain of 15%. These tubes were instrumented with optical fiber and 30 mm long electrical resistance strain gauges for validation purposes. The sensor fiber is nylon coated standard single mode optical fiber with diameter of 0.9mm, no slippage was observed between the nylon and the fiber in the range of use of the fiber. Four longitudinal lines of optical fiber were glued at the tube cross-section positions defined by $z = \pm d/2$ and $y = \pm d/2$ in the PVC tube surfaces as shown in Fig. 2. Optical fiber is glued to the PVC tubes by the use of epoxy glue applying a tensile force that approximately

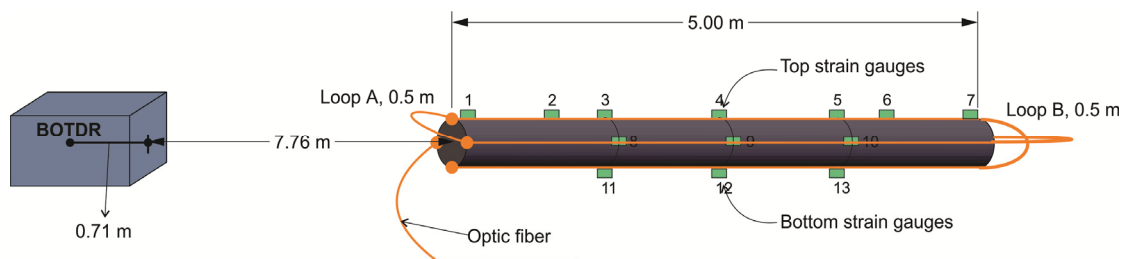


Fig. 3 Fiber optic mapping and strain gauges distribution

corresponds to a strain of 0.1%. There are 3 loops between optical fiber lines (Fig. 2) of approximately 0.5 m length to avoid large signal losses. No compensation for temperature was applied as it was verified that changes in temperature during testing were lower than the fiber error (i.e., 0.01%) given by the fabricant of the BOTDR equipment; however this compensation should be considered for an actual mine as discussed later in the paper. On the other hand, strain gauges (PFL-20-11, TML) give local measurements of longitudinal strain on the upper, lower and a lateral face of the PVC tubes, providing a strain resolution of 0.01% (similar to the value given by the optical fiber). Strain gauges were installed slightly rotated relative to the optical fiber as depicted in Fig. 3, which also shows their distribution along the length of the tube.

2.2 Laboratory tests

Four types of controlled relative displacements were applied to the ST supports (A, B, P1, and P2 in Fig. 4), which were believed to characterize the most likely rock mass movements due to mining operations. The distance between supports A and P1 and P2 and B is equal to 1.5 m and between P1 and P2 is equal to 2 m (Fig. 4). These supports are materialized with wood pedestals over which the ST is fixed using metal clamps (Fig. 2). The induced relative supports displacements were monotonically applied and the axial strains were measured using strain gauges and the BOTDR equipment. The magnitudes of these relative supports displacements were defined by treating the ST as a one-dimensional linear three-span continuous beam over two internal supports (P1 and P2 in Fig. 4) with Bernoulli's kinematic hypothesis (Popov 1998, McGuire *et al.* 2000; among others). Accordingly, a range of values of combination of relative supports displacement values, related to the expected rock mass displacement values, can be established in order to induce longitudinal strains on the ST that are greater than the error measurement of the optical fiber (0.01%).

A description of the induced relative ST supports displacements along with a sketch of them are presented below and in Fig. 4:

- Type I: vertical (in plane) displacement of point P1 (v_{yP1}).
- Type II: vertical and horizontal (out of plane) displacement of point P1 (v_{yP1} and v_{zP1} respectively).
- Type III: horizontal displacement of point P1 (v_{zP1}).
- Type IV: vertical displacement of points A and P1 (v_{yA} and v_{yP1} respectively).

In total, 18 tests were performed on tubes of length equal to 5.0 m. Half of these tests were carried out on 40 mm external diameter tubes and the other half on 25 mm diameter tubes. By treating the ST as one-dimensional linear beam member as previously discussed, tubes with different diameters allow recording rock mass displacements of diverse magnitudes accounting for the strain measurement error of the fiber: a 25 mm diameter tube is more flexible than a 40 mm diameter tube; thus smaller rock mass displacements would be better captured by the latter tube because greater longitudinal strains are induced in this tube, which can exceed the strain threshold value defined by the associated error of the fiber. Thus, small rock mass movements can be appropriately detected (i.e., axial strain values greater than the error of the optical fiber) by larger diameter sensors which was experimentally and numerically verified during the 25 mm and 40 mm diameter tubes experimental program and modeling the STs as a one-dimensional linear beam member respectively. Details about the measurements and numerical simulations can be found in Sotomayor (2013).

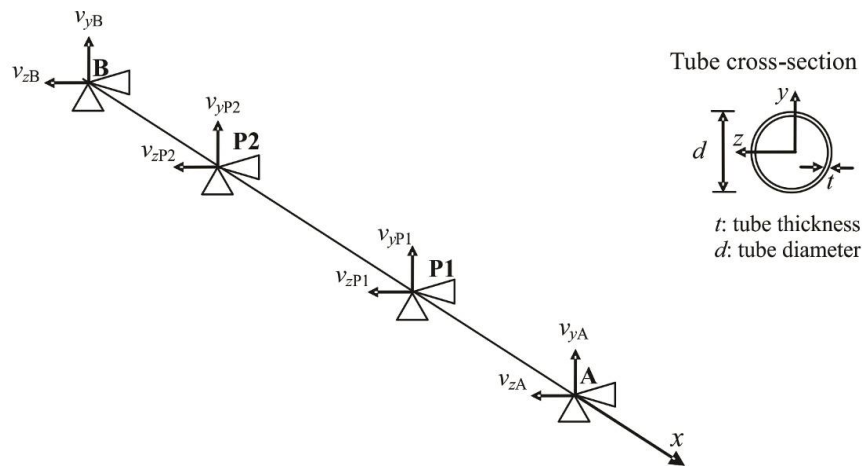


Fig. 4 ST supports displacements considered during experimental program

In order to illustrate the distribution of the axial strain along the ST induced by their relative supports displacements, results for a 40 mm diameter tube subjected to test type IV pattern are shown in Fig. 5. In this particular test type, the same vertical (y direction) displacements are prescribed for supports A and P1, which in this case range from 10.5 mm to 50 mm, while the other two supports (B and P2) are kept fixed. Only the strains measured by the upper ($y = d/2$) and lower ($y = -d/2$) fibers (yellow dots in the figure) are presented in this figure because the other two fiber lines ($z = \pm d/2$) do not record strain values. This implies that displacements in the y (vertical) direction do not induce axial strains at $z = \pm d/2$ (horizontal) locations; thus axis z - z is the neutral axis for displacements in the y direction. In addition, the measured strains vary in a sinusoidal fashion along the length of the ST indicating that the ST experiences curvature changes in its deformed configuration (bending behavior of the ST). The values measured by the optical fiber are in good agreement with those of the gauges (SG in the plot), with the exception of some of the values near the tube supports, although they are in the error range as previously commented. Additionally, predicted axial strains based on the linear beam theory (Popov 1998) are also shown in the plot. To this end, the following assumptions are made: (1) PVC has a linear-elastic response; (2) small deformation-based formulation; and (3) weight of the tube is considered negligible. The sensor is discretized into three two-noded one-dimensional elements that deform in bending (the so-called beam element), where each node of the element coincides with each sensor supports (points A, B, P1, and P2). Using a standard structural analysis procedure (McGuire *et al.* 2000), and considering the relative support displacements as the external static actions applied to the ST, its deformed configuration along with the associated normal stress and strain fields are computed (Sotomayor 2013).

For the particular case of the test type IV, a theoretical linear strain distribution compares well with measured values for regions between sensor supports. In the vicinity of the sensor supports (points A, B, P1 and P2), theoretical values deviate from measured values due to the Saint-Venant's principle. In this particular application, this principle establishes that the reaction forces developed at the ST supports locally (i.e., near the sensor supports) affect the stress and strain distributions given by linear beam theory. The results given by test type IV were selected to be shown because their results can be represented as a linear combination of test types I, II, and III

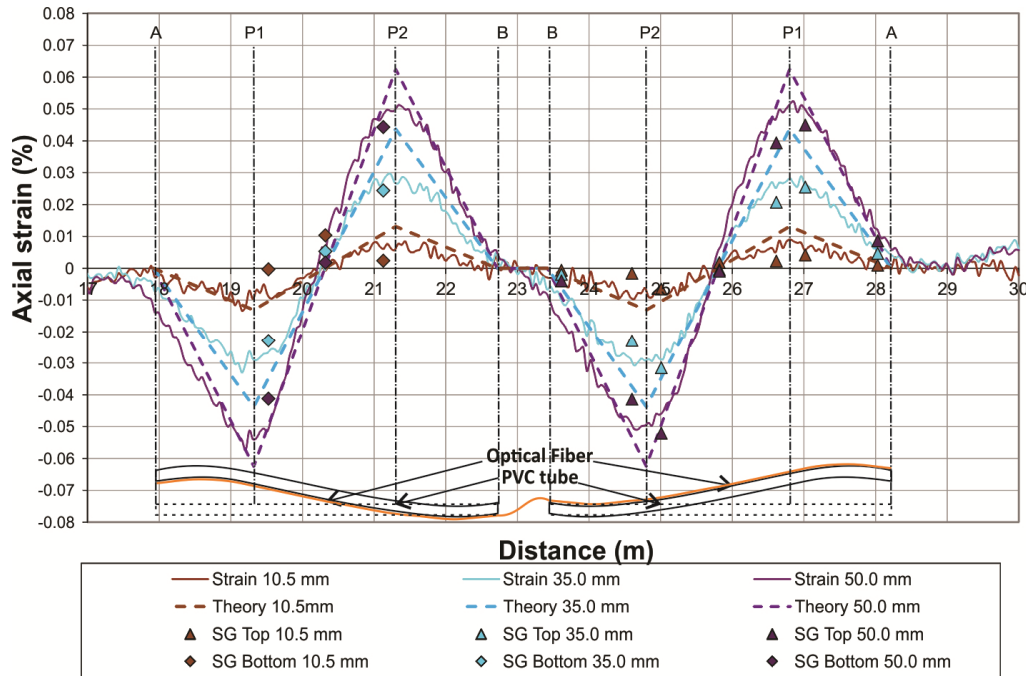


Fig. 5 Measured and theoretical strain values for test type IV on 40 mm diameter tube

provided that strains induced by vertical and horizontal displacements are uncoupled. Thus, for the range of support displacements used in this experimental study, linear beam theory also predicts in a satisfactory manner strain distributions associated with the latter test types.

2.3 Field tests

The proposed sensor (i.e., identical to the prototype used in the laboratory tests) was used in a field trial in underground tunnels of a mine to monitor deformation due to mining activities. The mine is located close to the city of Santiago (capital city of Chile), at an altitude of 2300 m above sea level in the Andes mountains and the STs were installed in tunnels that lay at an altitude close to 1900 m. In this particular tunnel monitoring, the sensors were constructed using a 40 mm diameter PVC tube of 5 m length. The attachment of the sensor to the rock was performed using a steel bolt glued to the rock with grout obtaining a rigid and superficial connection to the rock at each support point as simulated in the setup of the laboratory tests. The same type of metal clamps used to attach ST specimens in the lab was utilized to connect the steel bolts to the ST in the field. The installation is relatively fast and simple, but requires fusion of the optical fiber in the field (between the sensor and transmitting fiber) and this can be difficult and time consuming in underground field conditions (Fig. 6). A loop of fiber was used to compensate for temperature changes as successfully utilized previously on field measurements by Naruse *et al.* (2007).

Fig. 7 shows one example of preliminary measurements performed during a three month (October- December) field trial of a particular sensor installed in a tunnel of the underground mine. This sensor is located approximately 1.4 km away from the BOTDR equipment. Noticeable strain values, especially in the vertical plane (xy plane in Fig. 4) with values greater than 0.05% were



Fig. 6 Sensor tubes attached to the tunnel sidewall

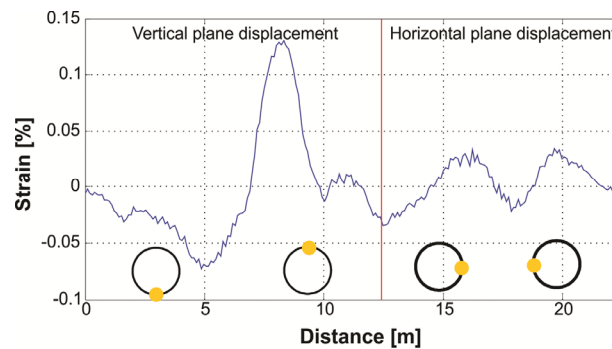


Fig. 7 Net strains induced to the sensor tube due to maintenance operations

measured by the upper and bottom fiber (yellow dots) of the ST. These measurements are associated to a maintenance procedure in which the ST was manipulated (vertical and lateral displacements exerted on the tube) inducing a bending deformation on it in both planes (sinusoidal strain distribution along the tube length). These preliminary measurements verified that the sensor was adequately connected to the BOTDR equipment and showed that the proposed ST can eventually detect other sources of strains in addition to rock mass movements, such as accidental damage and impacts due to operational mining activities.

3. Monitoring of anchors

Monitoring rock anchors in tunnels has become very important as the safety of many mining tunnels depends directly on them. The use of optical fiber serves as a method to monitor the performance of the steel anchors at a safe distance from the monitored point. Fig. 8(a) shows a schematic diagram of how the anchors work on the field. An experimental concrete slab (see Figs. 8(b)-(c)) was constructed in order to study whether the optical fiber is capable of representing the working condition of the anchor using the BOTDR technique.

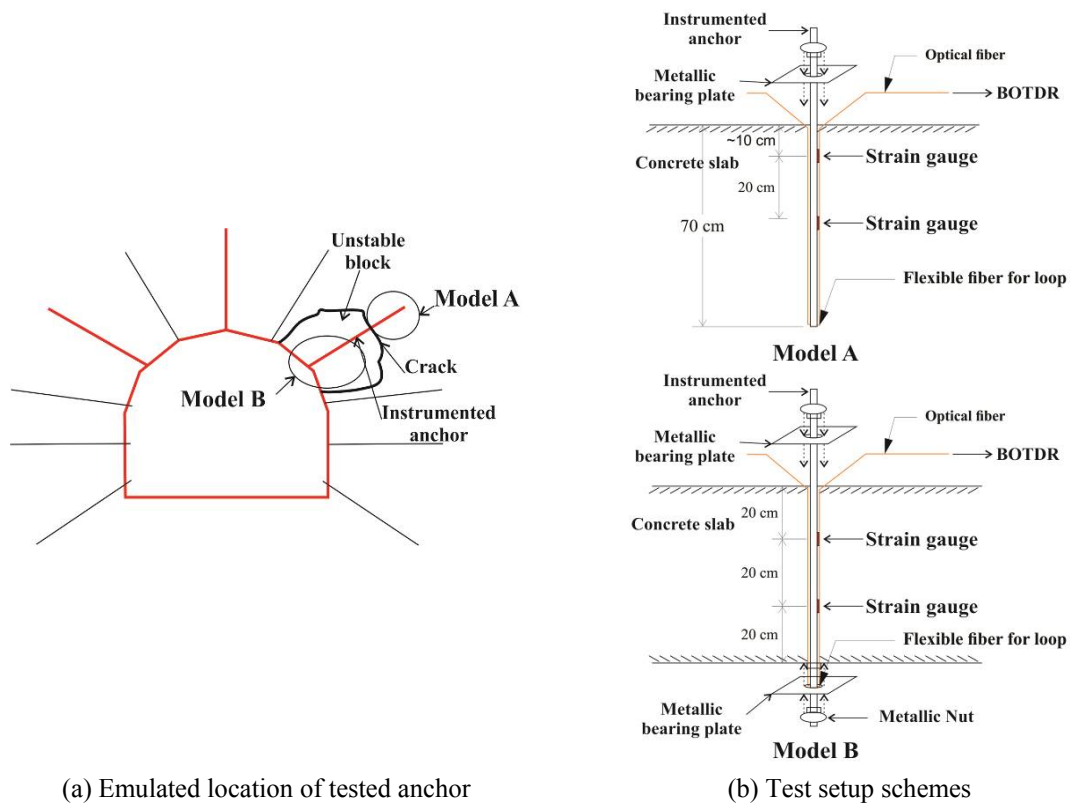


Fig. 8 Anchor testing details

The main problem when using the BOTDR technique with this type of anchor is that the length of the anchor can be only 2 to 3 m and the strain along the anchor is not constant. Therefore, to be able to obtain a reasonable measure of the strain in the anchor it is necessary to read directly the frequency domain as shown in Fig. 9. It is observed in this figure that there is not one well defined peak associated with the strain in the optical fiber, but rather two similar values. That means that part of the fiber is subjected to a strain different to the strain of the rest of the section. Under this

condition, the equipment will calculate the strain considering only one of the peaks (marked with a solid line), introducing an error in the value reported.

This problem can be overcome by integrating the curve of frequency in the range of the peaks of interest and calculating an average frequency \bar{F} using Eq. (1).

$$\bar{F} = \frac{\sum_i F_i A_i}{\sum_i A_i} \quad (1)$$

Where A_i is the area below the curve Power versus Frequency, and F_i is its corresponding frequency.

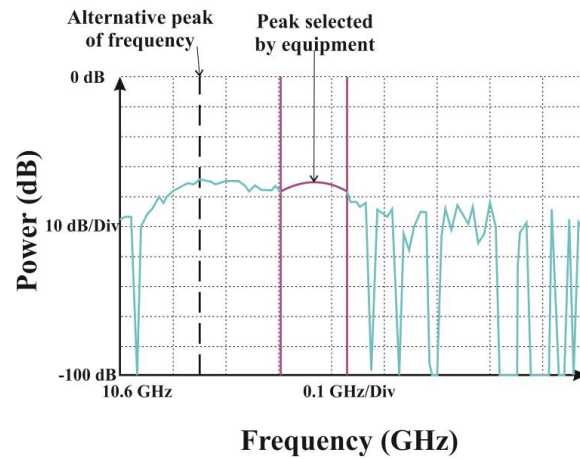


Fig. 9 Example of multiple peaks on the frequency domain under 150 kN of applied load to the anchor

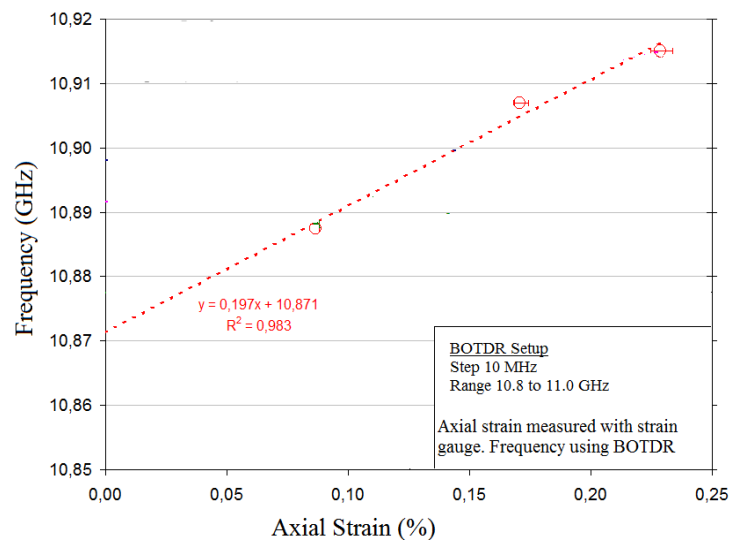


Fig. 10 Correlation between average frequencies and strains measured by strain gauge

The deduced average frequency in the anchor was compared with strain measurements obtained using strain gauges in the same point of the anchor, as it is shown for a particular case in Fig. 10. Noni *et al.* (2011) found also a correlation between the frequency shift and the strain in the fiber, obtaining a linear fit with a slope of 0.5. The difference with the slope of 0.2 found in this study can be explained because the equipment used to record the frequency shift, and the technique used to relate the frequency shift to strain are all different from what was used by Noni *et al.* (2011). It is also possible to deduce a correlation between measurements performed by using the BOTDR optical fiber and the actual strain in the anchor. This leads to the use of this technique to monitor the actual working condition of an anchor on the field during mining operations. Additional information about how to deduce the strain on the optical fiber in this case can be obtained from Sandoval (2010). This method shows to be useful to obtain an approximate state of the anchor, and therefore, it could be considered a maximum safe value of average frequency where the anchor is considered to be working properly.

4. Measurement of shotcrete deformations

Shotcrete is used often in tunnels as a secondary method of protection. This material is a mixture of water, cement, and fine aggregates (a type of concrete) with the high workability and fluidity required by the method of placing. This high resistance layer is sprayed against the rock face to help prevent the fall of rock blocks, which may be loose or broken between the anchors, forming a crust that increases the overall strength of the rock tunnel. The design of the shotcrete layer must consider aspects such as the strength of the shotcrete and the energy absorption capability. The standard test ASTM C1550 (2012) provides a useful method to evaluate the maximum strength and energy absorbed by the shotcrete. Fig. 11 shows a schematic plan view of the test configuration used in the tests conducted as part of the research reported in this paper.

A total of 23 shotcrete specimens were sprayed in the field to achieve a target thickness of 75 mm. All the shotcrete specimens were instrumented with optical fiber; however two suffered damage during spraying of the shotcrete on the mold or during transportation. Three configurations of fiber attachment were used in the 21 remaining specimens: 10 with “free” fiber, 10 with the fiber embedded in the shotcrete, and 1 with a combination of the two configurations. The scheme of the installation of the fiber on the shotcrete specimen for the “free” mode is shown in Fig. 10(a); the fiber is placed along two perpendicular diameters of the disc. In this mode, the fiber is first placed inside a plastic hose placed in the mold, then it is slightly prestressed between two fixed points at the ends of the hose, and finally the shotcrete is sprayed on the mold. Therefore, the fiber is unbonded from the surrounding shotcrete between these two points as shown in Fig. 12(a). Consequently, the strain can be estimated using Eq. (2).

$$\varepsilon = \frac{\sqrt{R^2 + \Delta^2} - R}{R} = \sqrt{1 + \left(\frac{\Delta}{R}\right)^2} - 1 \quad (2)$$

where R is the distance from the fixed point to the center of the disc, and Δ is the maximum vertical deflection of the disc.

On the other hand, the embedded optical fiber (see Fig. 12(b)) is bonded to the shotcrete along the entire length inside the specimen. In this case, the fiber is also placed along two perpendicular diameters of the disc, but each diameter has two branches looped around it. As explained before,

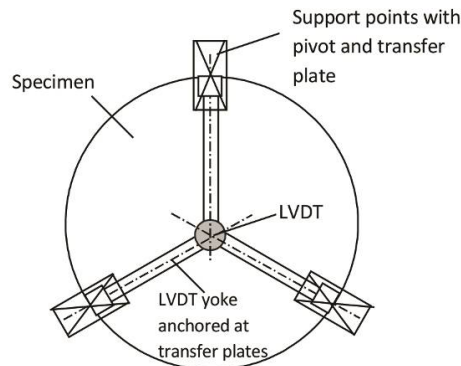


Fig. 11 Schematic of plan view of shotcrete disc and support points based on ASTM C1550 (2012)

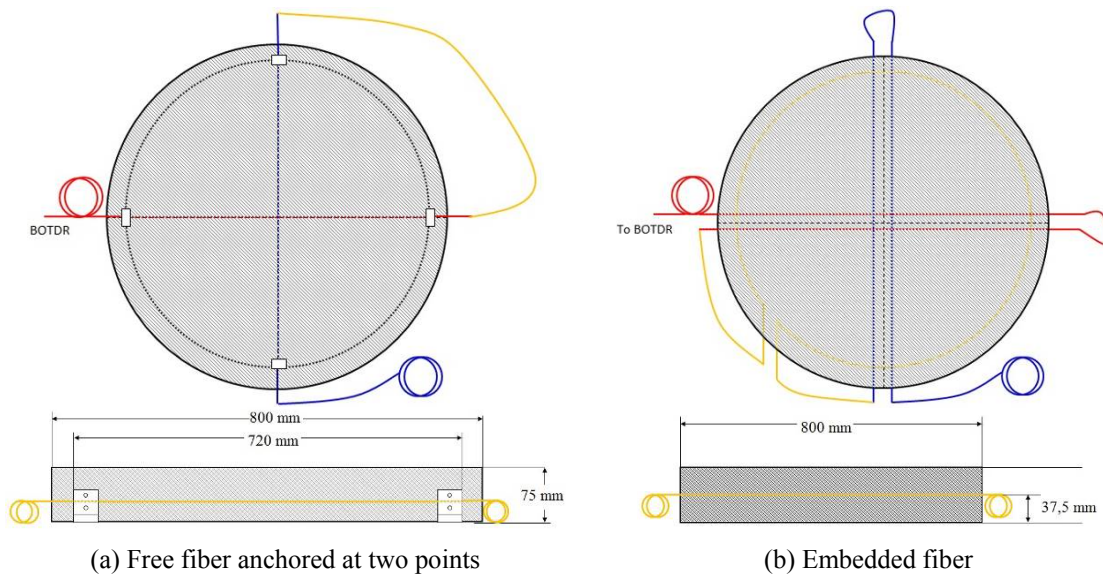


Fig. 12 Instrumented shotcrete discs

the optical fiber measures the change in frequency as an average in a distance of 1 m. Therefore, in this case the strain measured is only approximately equal to the actual value on the shotcrete disk. The difference between the deduced and actual values depends on the magnitude of the strain and length of the fiber subject to strain as explained by Hao and Wu (2008) and Ohsaki *et al.* (2002).

4.1 Test procedure

Every test was conducted according to ASTM C1550 (2012), but with one important difference: the deformation at the center of the disc was applied under a constant rate of 4 mm/min \pm 1 mm/min, as specified by the standard, but the deformation was paused for a period of about 5 minutes at each sampling point, to allow for the time required for the BOTDR to obtain its measurements. This pause was also used to measure crack openings during testing. All the

specimens were tested not less than 3 weeks after in-situ preparation.

4.2 Results of the measurements on shotcrete

Fig. 13 shows an example of the strains measured during testing of one of the “free” fiber specimens. The relative strain is calculated by subtracting from the strain measurement at any load or deformation stage, the strain measured at the beginning of the test.

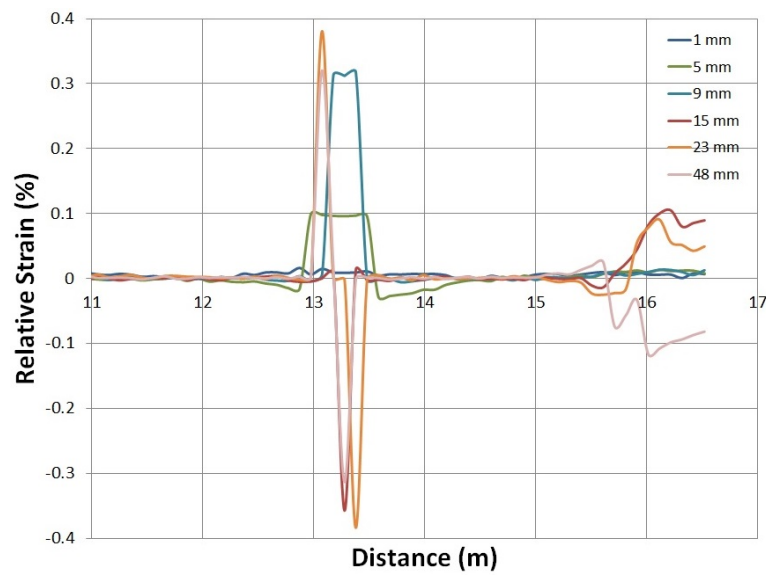


Fig. 13 Strain measurements with the optical fiber, specimen IC-1

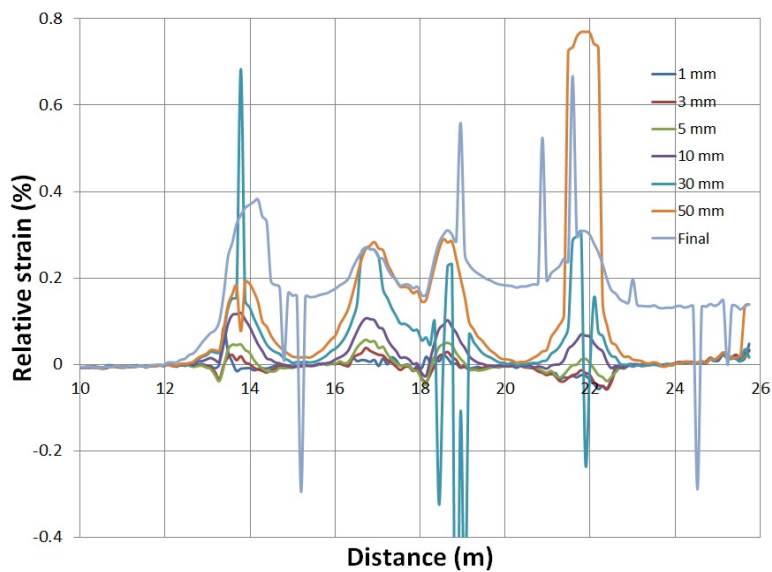


Fig. 14 Relative strain on the optical fiber BOTDR- test 9EMB

When the applied displacement is in the order of 1 to 3 mm, no strains are detected by the optical fiber. At a displacement of 5 mm, a strain in the order of 0.1% is detected in the first fiber that crosses the specimen. This threshold is consistent with the limit of 5 mm used in practice to mark the deformation at which the shotcrete loses its impermeability due to the formation of cracks. In the tests, visible cracks are not observed until approximately 10mm of displacement. Strains measured at applied vertical displacement of 5 and 9 mm show a clear zone with tensile strain due to the flexure of the specimen. For vertical displacements between 15 and 48 mm, it is observed that tension and compression is measured in the optical fiber. This could be due to the bending of the disc that may induce shear along the fiber. A maximum strain of approximately 0.4% is detected in test IC-1, when a vertical displacement of 23 mm is applied.

It can be concluded, from this example and the other measurements, that it is possible to obtain adequate strain measurements using the “free” fiber technique from the moment at which the crack openings start to develop and the shotcrete is therefore no longer impermeable. Also, in principle, it should be possible to correlate the strain measured and the energy absorbed to define a limit of serviceability on the field.

Similarly, an example of the strain measurements obtained on a specimen with the embedded optical fibers is given in Fig. 14. This figure shows graphs of the relative strains deduced during the tests. It is seen that the location where the embedded fiber is in contact with the shotcrete coincides with the places where strain measurements are obtained.

In this case, using the embedded fiber, the strains obtained are smaller in magnitude than those observed before with the “free” fiber. However, strains are now measured for vertical applied deformations as low as 3 mm and in a more continuous manner along the fiber. For an applied 5 mm vertical displacement, the strain measured with the optical fiber is in the order of 0.04% (compared with the 0.1% in the previous tests). Strains up to approximately 0.8% were measured for a 50 mm applied vertical displacement. Therefore, this technique also demonstrates to be useful to detect deformation in the shotcrete, and a relationship can be developed to relate the absorbed energy or developed strength with the strains measured with the optical fiber.

The feasibility of relating strains measured with the BOTDR with transverse deformation of the shotcrete was studied, with the intention of exploring the use of the fiber in the shotcrete to detect movements or deformations of the tunnel wall. Fig. 15 shows the relationship between the strains measured with the fiber (BOTDR) and the applied vertical displacement for the “free fiber” specimen. Similarly, Fig. 16 illustrates the relationship between the strains measured using the BOTDR and the applied vertical displacement when the fiber is embedded in the shotcrete. In both cases there is a similar maximum envelope. However, there are points that escape this envelope due to what seems to be consequence of damage during transportation of the shotcrete discs from the field to the laboratory. In the case of the free fiber sensor, there were more discs with clear cracks before testing, which is reflected in a larger number of points above the proposed envelope.

In addition to the effect of minor damage during transportation, part of the difference can be attributed to other factors such as the orientation of the fiber with respect to the support points. In order to evaluate this effect, a numerical model, shown in Fig. 17, was constructed in ANSYS to reproduce the behavior in the elastic range of the specimens tested. The model considered a homogeneous linear elastic material for the shotcrete, neglecting the contribution of the fiber stiffness. Fig. 17 shows the difference in the strains calculated along three different diameters in the disc. With the exception of the discontinuities near the support points, the strains are essentially the same along the three diameters, and the maximum tensile strains are concentrated around the center of the disc. Therefore, the significant variability in the initial measurements

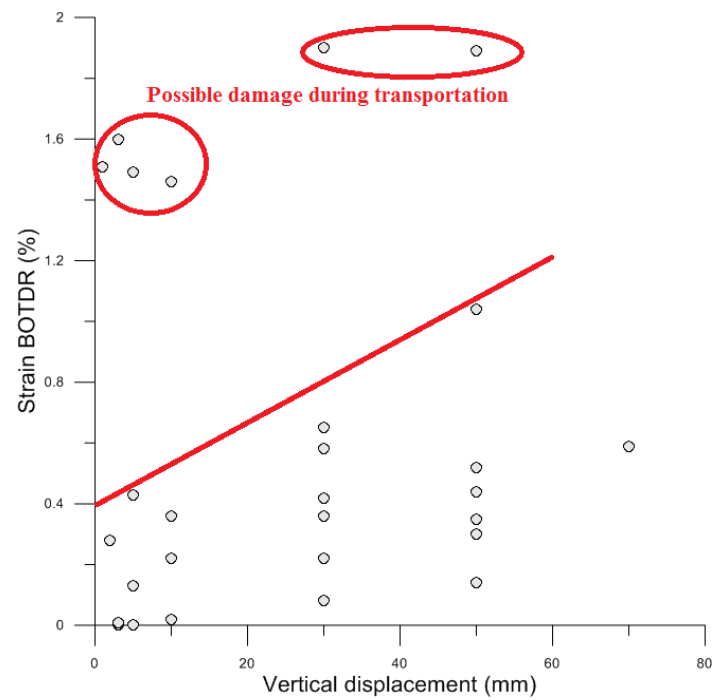


Fig. 15 Relationship between strain BOTDR and applied deformation "free fiber sensor"

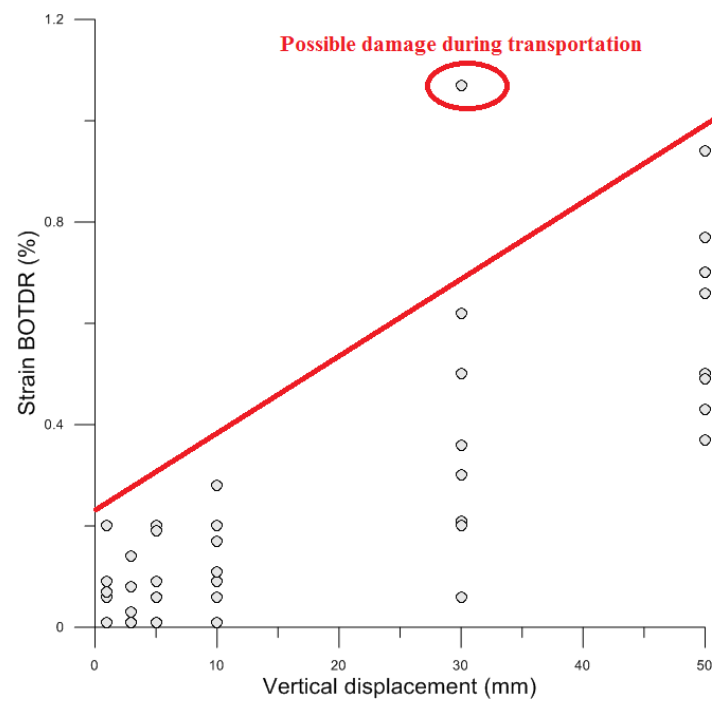


Fig. 16 Relationship between strain BOTDR and applied deformation "embedded fiber sensor"

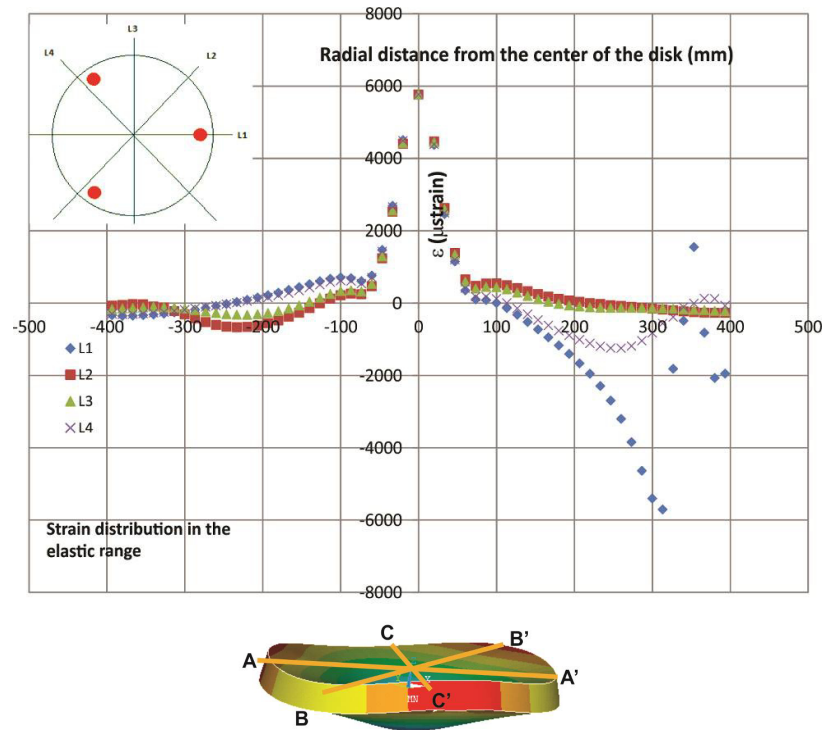


Fig. 17 Strain distribution derived through numerical model of the disk during the linear elastic range

during the test, associated to the smallest displacements, has a negligible influence from the orientation of the fiber. In consequence, the differences are due mainly to damage during transportation of the shotcrete disks from the field.

In summary, optical fiber measurements of strains using the BOTDR can be obtained and the state of the shotcrete ascertained from the recorded strains. However, more reliable measurements of strains can only be achieved after small cracks are formed, and even in this case, there is significant scatter in the measured strains believed to be due mainly to the damage that the shotcrete disk may have at the beginning of the test. In the field, this scatter is expected to be lower as the shotcrete is poured in place with no transportation involved.

Although the length of the fiber subjected to strain (0.7 and 0.8 m depending on the tests) is less than the spatial resolution of the measurement of 1.0 m, the correction to the actual value of strain would be null for strains larger than 0.25%, and less than 30% for strains lower than 0.25% (Hao and Wu 2008).

5. Conclusions

Three different mining applications of structural monitoring using optical fiber are presented in this paper. The following conclusions are drawn regarding the feasibility and performance of these monitoring applications:

- An instrumented PVC tube using optical fiber shows that is possible to measure strains

along the tube induced by relative displacements of its support points. Laboratory tests and theoretical analysis confirm its functionality.

- Field trials at the interior of a mine tunnel show that it is possible to detect displacements events that induce strains along the tube sensor.
- Tube sensors prove to be easy to install and implement in the interior of rock tunnels.
- Field tests show that it is possible to detect strains that occur in a rock anchor using an average value of the frequency measured along the anchor. In addition, strains in the anchors can be correlated with the average strains obtained using the optical fiber.
- Two different configurations of instrumented shotcrete discs are tested in the laboratory. In both configurations it is possible to measure strains along the shotcrete and correlate the strain values with the state of the shotcrete. Strain measurements are only meaningful up to the point when the first cracks appear in the shotcrete. This conclusion is supported by numerical simulations.

References

- ASTM C1550 (2012), Standard Test for Flexural Toughness of Fiber Reinforced concrete (Using Centrally Loaded Round Panel); ASTM C1550 – 12a, West Conshohocken, PA, USA.
- Cheung, L.L.K., Soga, K., Bennett, P.J., Kobayashi, Y., Amatya, B. and Wright, P. (2010), “Optical fibre strain measurement for tunnel lining monitoring”, *Proceedings of the Institution of Civil Engineers, Geotechnical Engineering*, **163**(GE3), 119-130.
- Gage, J.R., Fratta, D., Turner, A.L., MacLaughlin, M.M. and Wang, H.F. (2013), “Validation and implementation of a new method for monitoring in situ strain and temperature in rock masses using fiber-optically instrumented rock strain and temperature strips”, *Int. J. Rock Mech. Mining Sci.*, **61**, 244-255.
- Hao, Z. and Wu, Z. (2008), “Performance evaluation of BOTDR-based distributed fiber optic sensors for crack monitoring”, *Struct. Health Monitor.*, **7**(2), 143-156.
- Horiguchi, T., Kurashima, T. and Tateda, M. (1989), “Tensile strain dependence of brillouin frequency shift in silica optical fibers”, *IEEE Photon. Technol. Lett.*, **1**(5), 107-108.
- Inaudi, D. and Glisic, B. (2010), “Long-range pipeline monitoring by distributed fiber optic sensing”, *J. Press. Vessel Tech.*, **132**(1), 0117011-0117019.
- McGuire, W., Gallagher, R. and Ziemian, R. (2000), *Matrix Structural Analysis*, (Second Edition), John Wiley & Sons, Inc., Hoboken, NJ, USA.
- Mohamad, H., Soga, K., Bennett, P.J., Mair, R.J. and Lim, C.S. (2012), “Monitoring twin tunnel interaction using distributed optical fiber strain measurements”, *J. Geotech. Geoenviron. Eng.*, **138**(8), 957-967.
- Naruse, H., Uehara, H., Deguchi, T., Fujihashi, K., Onishi, M., Espinoza, R., Guzman, C., Pardo, C., Ortega, C. and Pinto, M. (2007), “Application of a distributed fibre optic strain sensing system to monitoring changes in the state of an underground mine”, *Meas. Sci. Technol.*, **18**(10), 3202-3210.
- Nikles, M., Burke, R., Briffod, F. and Lyons, G. (2005), “Greatly extended distance pipeline monitoring using fibre optics”, *Proceedings of the International Conference on Offshore Mechanics and Arctic Engineering - OMAE*, **3**, 539-546.
- Noni, MacLaughlin, M.M. and Wang, H.F. (2011), “Validation of fiber-optic strain-sensing cable for deep underground installation”, *Proceedings of the 45th US Rock Mechanics Symposium*, San Francisco, CA, USA, June.
- Ohno, H., Naruse, H., Kihara, M. and Shimada, A. (2001), “Industrial applications of BOTDR optical fiber strain sensor”, *Opt. Fib. Tech.*, **7**(1), 45-64.
- Ohsaki, M., Tateda, M., Omatsu, T. and Ohno, H. (2002), “Spatial resolution enhancement of distributed strain measurement using BOTDR by partially gluing optical fiber”, *IEICE Transact. Communications*,

E85-B(8), 1636-1639.

Popov, E. (1998), *Engineering Mechanics of Solids*, (Second Edition), Prentice Hall, Upper Saddle River, NJ, USA.

Sandoval, J. (2010), "Spatial resolution of optical fiber measurements in rock bolts for mining tunnels", Master's Thesis; University of Chile, Santiago, Chile. [In Spanish]

Shimizu, N., Nakashima, S. and Masunari, T. (2014), "ISRM suggested method for monitoring rock displacements using the global positioning system (GPS)", In: *The ISRM Suggested Methods for Rock Characterization, Testing and Monitoring: 2007-2014*, (Ulusay, R. Ed.), Springer International Publishing, Cham, Switzerland.

Sotomayor, J. (2013), "Plataforma computacional para el análisis de un sensor de desplazamiento de túneles", Engineering Thesis; University of Chile, Santiago, Chile. [In Spanish]

Sun, Y., Shi, B., Chen, S., Zhu, H., Zhang, D. and Lu, Y. (2014), "Feasibility study on corrosion monitoring of a concrete column with central rebar using BOTDR", *Smart Struct. Syst., Int. J.*, **13**(1), 41-53.

Thévenaz, L., Niklès, M., Fellay, A., Facchini, M. and Robert, P.A. (1998), "Truly distributed strain and temperature sensing using embedded optical fibers", *Proceedings of SPIE - Smart Structures and Materials 1998*, San Diego, CA, USA, March, Volume 3330, pp. 301-314.

Vinilit, www.vinilit.cl

CC